

Optical levitation of microdroplet containing a single quantum dot

Y. Minowa¹, R. Kawai¹, & M. Ashida¹

¹*Graduate School of Engineering Science, Osaka University, Toyonaka, Osaka 560-8531, Japan*

Semiconductor nanocrystals, also known as quantum dots (QDs), are key ingredients in current quantum optics experiments. They serve as quantum emitters¹ and memories² and have tunable energy levels that depend not only on the material but also, through the quantum confinement effect, on the size³. The resulting strongly confined electron and hole wave functions lead to large transition dipole moments^{4,5}, which opens a path to ultra strong coupling and even deep strong coupling between light and matter^{6,7}. Such efficient coupling requires the precise positioning⁸ of the QD in an optical cavity with a high quality factor and small mode volume, such as micro-Fabry–Perot cavity⁹, whispering-gallery-mode microcavity¹⁰, or photonic-crystal cavity¹¹. However, the absence of a technique for free-space positioning has limited the further research on QD-based cavity quantum electrodynamics. In this paper, we present a technique to overcome this challenge by demonstrating the optical levitation or trapping in helium gas of a single QD within a liquid droplet. Bright single-photon emission from the levitated QD was observed for more than 200 s. To the best of our best knowledge, this study provides the first proof-of-principle demonstration of an optically levitated solid-state quantum emitter.

Optical traps, optical tweezers, or optical dipole traps are ubiquitous techniques^{12,13} that are

widely used in fields such as molecular biology, chemistry, and physics. These techniques have formed the foundation of single-molecule research. For example, micrometer-sized beads optically trapped in room temperature liquid have been used as a handles to manipulate DNA, RNA, and molecular motors¹⁴. Optical trapping is also indispensable for capturing, aligning and cooling cold atoms¹⁵. Far-off-resonance optical dipole traps, together with optical cavities, provides a rich playground for studying the interaction between single atoms and single photons¹⁶. The longest trapping lifetime reported to date for a single atom is ~ 100 s¹⁷, which is sufficiently long to demonstrate coherent state manipulation in the strong coupling regime¹⁵.

The attainment of the strong-coupling regime requires an optical cavity with a high quality factor and a small mode volume, a large transition dipole moment and precise free-space positioning of the dipole with respect to the cavity. The requisite free-space positioning has been attained using an optical dipole trap⁸. Thus, combining an optical dipole trap with a much larger transition dipole moment should result in ultra strong coupling, or even deep strong coupling, enabling us to further investigate novel quantum-optics phenomena^{6,7}.

A large transition dipole moment is available from collective excitations in condensed matter systems, and solid-state semiconductor nanocrystal (i.e., QDs), which are very stable quantum emitters, exhibit such collective excitation in the form of excitons³. Through the quantum confinement effect, the material from which QDs are made and their shape and size determine the QD energy levels. The strong confinement provided by QDs also enhances the transition dipole moment⁴. Of the many types of the QDs, chemically synthesized colloidal QDs are well-suited for this application as their size can be controlled with precision, they are photostable ,and they

can be mass produced³. Colloidal QDs act as a single isolated entity and several groups have reported on optically manipulating and trapping colloidal QDs in liquid¹⁸. However, no report that demonstrates optical levitation^{19,20} or optical trapping of a single QD in gas or vacuum has yet appeared.

To obtain stable optical levitation of a single QD, a major obstacle is the small nonresonant polarizability of the QD. In the Rayleigh regime $r \ll \lambda$, the nonresonant polarizability α of a particle with radius r is proportional to the volume¹⁸ $\alpha \propto r^3$. Consider CdSe/ZnS core/shell colloidal QDs as an example; the typical polarizability in the transparent region is $\alpha/\epsilon_0 \sim 2.6 \times 10^{-25} \text{ m}^3$. If a high-power (1 W), 785 nm Gaussian beam is focused via an "ideal" lens²¹, the trap depth would be very close to room temperature, which is insufficient for stable trapping (see Supplementary Information). The most plausible way to circumvent this problem is to embed the single QD into a larger volume of transparent material. In the present study, we demonstrate that a strong single-beam gradient force can optically levitate a single CdSe/ZnS core/shell QD embedded in a micrometer-sized liquid droplet in helium gas. The microdroplet is easy to produce and handle and is highly symmetric, making it well suited for stable optical levitation.

Using a strongly focused near-infrared laser beam, we optically levitated an ethanol microdroplet containing a chemically synthesized CdSe/ZnS QD. Figure 1 shows the experimental setup. The laser power after the objective lens was 1.4 W, which is sufficient for the stable optical levitation of the micrometer-sized ethanol droplet. The ethanol microdroplets were introduced into the sample chamber via an ultrasonic nebulizer¹⁹. Inside a sample chamber filled with helium gas, the trapping lifetime of the microdroplet exceeded several dozen minutes. The optical absorption

of the ethanol droplet has a negligible effect on the quantum efficiency of the fluorescence of the single QD (the absorption coefficient of liquid ethanol is $\sim 10^{-2} \text{ cm}^{-1}$ at 785 nm and $\sim 10^{-3} \text{ cm}^{-1}$ across the entire visible spectrum).

Through two-photon absorption, the trapping laser excited the optically levitated QD inside the droplet. CdSe/ZnS QDs have a large two-photon-action cross section, which is the product of the nonlinear two-photon-absorption cross section and the fluorescence quantum efficiency²². Based on the two-photon-action cross section, we estimated the maximum rate of photon emission to be $10^7 \sim 10^9$ photons/s (see Supplementary Information). The two-photon-excited fluorescence was split by a 50/50 beam splitter into two beams and coupled into multimode optical fibers (see Figure 1). The small fiber core (diameter 105 μm) provides a confocal pinhole and eliminates a large fraction of the stray light. The output of the two fibers was directed onto single-photon-counting avalanche photodiode modules. The Hanbury Brown and Twiss setup allows us to investigate the photon statistics of the levitated photon source. Figure 2 shows the measured two-photon coincidence counts $g^{(2)}(t)$ fit to an exponential function (solid line). If the levitated QD emits a single photon at a time, the photon coincidence at $t = 0$ would ideally go to zero. The observed small value of $g^{(2)}(t) = 0.22$ indicates that the optically levitated QD behaved as a single-photon source. The small offset remaining at $t = 0$ may be due to stray light, the finite time resolution of the detector, and the biexciton cascade decay²³. The time constant $\tau = 6.9$ ns obtained from the fit is related to the fluorescence lifetime τ_{decay} and the excitation rate Γ by $\frac{1}{\tau} = \frac{1}{\tau_{\text{decay}}} + \Gamma$ and is consistent with the previous studies^{24,25}.

The lower panel of Fig. 3 shows the temporal dynamics of two-photon-excited fluorescence

from a levitated QD. After recording the two-photon coincidence counts and ensuring the single-photon emission, one of the avalanche photo diodes was replaced by a spectrograph and the fluorescence was recorded with a 1 s integration time. The fluorescence line width is much narrower than that of the QD ensemble (see dotted blue curve in upper panel of Fig. 3), which indicates that inhomogeneous broadening has been eliminated. However, this line width 15.2 ± 0.2 nm may still include the effect of rapid spectral diffusion within the integration time²⁶. Moreover, the photoluminescence intensity evidently fluctuated during acquisition. To further examine the temporal change of the fluorescence dynamics, we recorded it using the avalanche photodiode (Fig. 4). The integration time was 20 ms/bin, and data were recorded over 200 s. The fluorescence intensity from the levitated QD strongly fluctuated on a sub-second-scale, reflecting the Brownian motion of the QD within the liquid droplet and the blinking characteristic, which is expected from single-QD fluorescence^{24,25}. The measured maximum photon counting rate was about 2×10^5 counts/s. Considering our detection efficiency of at most 6 %, we calculate that the photon emission rate during optical levitation exceeded $10^6 \sim 10^7$ photons/s. Such a high photon-emission rate is consistent with the value estimated above from the two-photon-action cross section and provides convincing evidence of bright single-photon emission. Although one may expect an enhanced spontaneous emission rate through the Purcell effect²⁷ (due to the presence of the ethanol micro-droplet), we saw no significant spontaneous emission enhancement. The fluorescence spectra also clearly show that no cavity mode is present.

Overall, our results shows that by exploiting the optical gradient force on a microdroplet containing a single QD, a focused laser beam can position a QD at a given position in free space.

To improve on these results, the internal temperature and center-of-mass motion of the levitated QD could be reduced by buffer-gas cooling²⁸ to suppress the decoherence, which significantly hinders the observation and control of the quantum states. In addition, stable optical levitation of a bare QD would become straightforward if the center-of-mass motion is reduced by cooling to sub-Kelvin regime. The current approach is also readily extendable to multistep optical levitation, whereby the QD-microdroplet system is optically levitated, followed by cooling to reduce motion and subsequent levitation of a bare QD in a shallow optical trap.

Finally, the experimental methods developed in this study can lead to optical levitation of a number of fascinating nanomaterials and their concomitant isolation from the substrate or matrix. Because of the large surface-to-volume ratio, the properties of nanomaterials tend to depend strongly on their environment^{29,30}, and environment-induced effects often impede the detailed study of the nanomaterials. Thus, optical levitation in gas or vacuum would provide an ideal platform to investigate nanomaterials and should lead to an improved understanding of their intrinsic properties.

Methods Summary

Sample preparation Core/shell type CdSe/ZnS QDs with an emission wavelength of 640 nm in toluene (Sigma Aldrich) were diluted to $1/10^3$ in ethanol. This solution was sonicated in an ultrasonic bath for 30 min before use. Ethanol microdroplets (refractive index 1.36) containing the QDs were sprayed from an ultrasonic nebulizer (Omron, NE-U22) into the sample chamber.

Experimental setup A continuous wave Ti:sapphire laser beam with a wavelength of 785 nm was

focused into a sample chamber after a laser line filter by a microscope objective with a numerical aperture of 0.9 (Olympus, UPFLN60X). The sample chamber was formed by two coverslips separated by a rubber O-ring (mounted with vacuum grease to prevent airflow) and was filled with helium gas. The O-ring had a cut through which the microdroplets containing single QDs were introduced. The fluorescence induced by two-photon-excitation was routed by a dichroic mirror (Semrock, FF740-Di01) and passed through bandpass filters to block scattered light. It was then focused by an 80-mm-focal-length lens and split into two beams by a 50/50 nonpolarizing beam splitter. Each beam was coupled into multimode fibers (Thorlabs, M43L01), whose core acted as a pinhole for confocal microscopy. The multimode fibers were connected to a spectrograph to monitor the fluorescence spectra or connected to single-photon-counting modules (Excelitas Technologies, SPCM-AQRH-14) to measure the second-order correlation function $g^{(2)}(t)$. Electronic pulses from the two single-photon-counting modules were used as start/stop signals for a time-to-amplitude converter system.

1. Müller, M., Bounouar, S., Jöns, K. D., Glässl, M. & Michler, P. On-demand generation of indistinguishable polarization-entangled photon pairs. *Nature Photonics* **8**, 224–228 (2014).
2. Hanson, R. & Awschalom, D. D. Coherent manipulation of single spins in semiconductors. *Nature* **453**, 1043–1049 (2008).
3. Trindade, T., O'Brien, P. & Pickett, N. L. Nanocrystalline semiconductors: Synthesis, properties, and perspectives. *Chemistry of Materials* **13**, 3843–3858 (2001).
4. Kayanuma, Y. Quantum-size effects of interacting electrons and holes in semiconductor mi-

- crocrystals with spherical shape. *Physical Review B* **38**, 9797–9805 (1988).
5. Thränhardt, A., Ell, C., Khitrova, G. & Gibbs, H. Anisotropic emission of interface fluctuation quantum dots. *The European Physical Journal B - Condensed Matter* **27**, 571–576 (2002).
 6. Stassi, R., Ridolfo, A., Di Stefano, O., Hartmann, M. J. & Savasta, S. Spontaneous conversion from virtual to real photons in the ultrastrong-coupling regime. *Physical Review Letters* **110**, 243601 (2013).
 7. De Liberato, S. Light-matter decoupling in the deep strong coupling regime: The breakdown of the purcell effect. *Physical Review Letters* **112**, 016401 (2014).
 8. Nußmann, S. *et al.* Submicron positioning of single atoms in a microcavity. *Physical Review Letters* **95**, 173602 (2005).
 9. Ye, J., Vernooy, D. W. & Kimble, H. J. Trapping of single atoms in cavity QED. *Physical Review Letters* **83**, 4987–4990 (1999).
 10. Verhagen, E., Deléglise, S., Weis, S., Schliesser, A. & Kippenberg, T. J. Quantum-coherent coupling of a mechanical oscillator to an optical cavity mode. *Nature* **482**, 63–67 (2012).
 11. Takahashi, Y. *et al.* A micrometre-scale raman silicon laser with a microwatt threshold. *Nature* **498**, 470–474 (2013).
 12. Grier, D. G. A revolution in optical manipulation. *Nature* **424**, 810–816 (2003).
 13. Ashkin, A. Acceleration and trapping of particles by radiation pressure. *Physical Review Letters* **24**, 156–159 (1970).

14. Moffitt, J. R., Chemla, Y. R., Smith, S. B. & Bustamante, C. Recent advances in optical tweezers. *Annual Review of Biochemistry* **77**, 205–228 (2008).
15. McKeever, J. *et al.* State-insensitive cooling and trapping of single atoms in an optical cavity. *Physical Review Letters* **90**, 133602 (2003).
16. Birnbaum, K. M. *et al.* Photon blockade in an optical cavity with one trapped atom. *Nature* **436**, 87–90 (2005).
17. He, J., Yang, B., Cheng, Y., Zhang, T. & Wang, J. Extending the trapping lifetime of single atom in a microscopic far-off-resonance optical dipole trap. *Frontiers of Physics* **6**, 262–270 (2011).
18. Jauffred, L., Richardson, A. C. & Oddershede, L. B. Three-dimensional optical control of individual quantum dots. *Nano Letters* **8**, 3376–3380 (2008).
19. Neukirch, L. P., Gieseler, J., Quidant, R., Novotny, L. & Nick Vamivakas, A. Observation of nitrogen vacancy photoluminescence from an optically levitated nanodiamond. *Optics Letters* **38**, 2976–2979 (2013).
20. Arita, Y., Mazilu, M. & Dholakia, K. Laser-induced rotation and cooling of a trapped micro-gyroscope in vacuum. *Nature Communications* **4** (2013).
21. Tey, M. K. *et al.* Interfacing light and single atoms with a lens. *New Journal of Physics* **11**, 043011 (2009).

22. Larson, D. R. *et al.* Water-soluble quantum dots for multiphoton fluorescence imaging in vivo. *Science* **300**, 1434–1436 (2003).
23. Nair, G., Zhao, J. & Bawendi, M. G. Biexciton quantum yield of single semiconductor nanocrystals from photon statistics. *Nano Letters* **11**, 1136–1140 (2011).
24. Yoshikawa, N. *et al.* Biexciton state causes photoluminescence fluctuations in CdSe/ZnS core/shell quantum dots at high photoexcitation densities. *Physical Review B* **88**, 155440 (2013).
25. Michler, P. *et al.* Quantum correlation among photons from a single quantum dot at room temperature. *Nature* **406**, 968–970 (2000).
26. Coolen, L., Spinicelli, P. & Hermier, J.-P. Emission spectrum and spectral diffusion of a single CdSe/ZnS nanocrystal measured by photon-correlation fourier spectroscopy. *Journal of the Optical Society of America B* **26**, 1463–1468 (2009).
27. Purcell, E. M. Spontaneous emission probabilities at radio frequencies. *Physical Review* **69**, 681 (1946).
28. Doret, S. C., Connolly, C. B., Ketterle, W. & Doyle, J. M. Buffer-gas cooled bose-einstein condensate. *Physical Review Letters* **103**, 103005 (2009).
29. Park, Y.-S. *et al.* Near-unity quantum yields of biexciton emission from CdSe/CdS nanocrystals measured using single-particle spectroscopy. *Physical Review Letters* **106**, 187401 (2011).

30. Zhao, H.-Q., Fujiwara, M. & Takeuchi, S. Effect of substrates on the temperature dependence of fluorescence spectra of nitrogen vacancy centers in diamond nanocrystals. *Japanese Journal of Applied Physics* **51**, 090110 (2012).

Acknowledgements We thank H. Ishihara, M. Kumakura, Y. Moriwaki, and T. Torimoto for their useful discussions. This study was partially supported by KAKENHI from the MEXT of Japan.

Author Contributions Y.M. conceived, initiated, and designed the project and wrote the paper. Y.M. and R.K. performed the experiments and analyzed the data. M.A. provided technical support and conceptual advice, as well as edited the manuscript.

Competing Interests The authors declare that they have no competing financial interests.

Correspondence Correspondence and requests for materials should be addressed to Y.M. (minowa@mp.es.osaka-u.ac.jp).

Supplementary Information:

The polarizability of a spherical particle is

$$\alpha = 4\pi\epsilon_0 \frac{\epsilon - 1}{\epsilon + 2} r^3, \quad (1)$$

where ϵ is the dielectric constant and r is the radius of the particle. The typical radius of CdSe/ZnS quantum dots (QDs) is 3.15 nm (Sigma Aldrich), and $\epsilon = 7.1$ at a wavelength of 785 nm. These values result in

$$\alpha/\epsilon_0 \sim 2.6 \times 10^{-25} \text{ m}^3. \quad (2)$$

Assuming an "ideal" lens is used to focus a Gaussian beam, the magnitude of the electric field at the focal point is [21]

$$E = \sqrt{\frac{\pi P}{\epsilon_0 c \lambda^2}} \frac{1}{u} e^{1/u^2} \left[\sqrt{\frac{1}{u}} \Gamma\left(-\frac{1}{4}, \frac{1}{u^2}\right) + \sqrt{u} \Gamma\left(\frac{1}{4}, \frac{1}{u^2}\right) \right], \quad (3)$$

where the incomplete gamma function $\Gamma(a, b) = \int_b^\infty t^{a-1} e^{-t} dt$, where P is the power of the Gaussian beam and λ is the wavelength. The parameter u indicates the focusing strength and is related to the focal length of the lens and the diameter of the incident beam. The electric field is maximum when the focusing strength is $u = 2.239$. With $P = 1 \text{ W}$ and $\lambda = 785 \text{ nm}$, we obtain a maximum electric field amplitude of $6.1 \times 10^7 \text{ V/m}$ at the focal point. The optical trap depth U_0 of a Rayleigh particle is given by

$$U_0 = \frac{1}{2} \alpha E^2. \quad (4)$$

With the values given above, $U_0 = 4.283 \times 10^{-21} \text{ J}$, which corresponds to 310 K.

The reported two-photon-action cross section is from 2000 to 50000 GM (using Goepfert-Mayer units[22]). The photon flux of the near-infrared laser is

$$\frac{c\epsilon_0}{2}E^2 \times \frac{1}{\hbar\omega} = 1.95 \times 10^{27} \text{ cm}^{-2}\text{s}^{-1}. \quad (5)$$

At the focal point, the expected rate of photon emission by fluorescence is thus 8×10^7 to 2×10^9 s^{-1} .

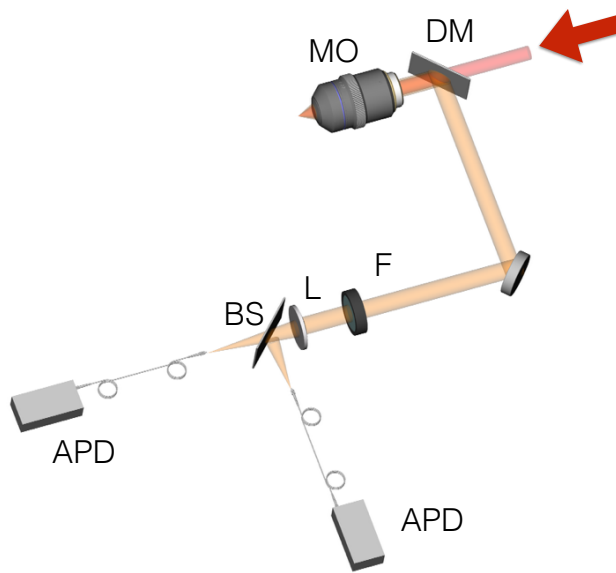


Figure 1 | Schematic of the experimental. Near-infrared light from a continuous-wave Ti:sapphire laser was focused using a microscope objective (MO). A dichroic mirror (DM) reflected two-photon-excited fluorescence from a levitated QD. To suppress stray light, we spectrally filtered the fluorescence using bandpass filters (F). Next, the fluorescence was focused by a lens (L) and split into two beams of equal intensity by a 50/50 beam splitter (BS). Each beam was coupled into multimode optical fibers and detected by avalanche photodiodes or a spectrograph. (see Methods Summary for details).

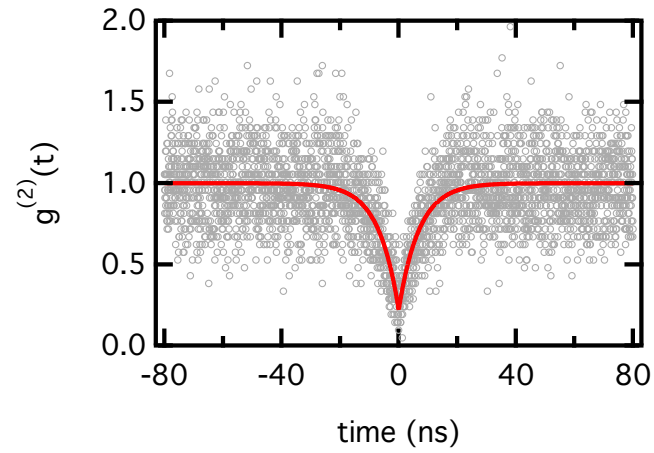


Figure 2 | Single levitated solid-state quantum emitter. Normalized second-order correlation function $g^{(2)}(t)$ of two-photon-excited single-QD fluorescence. The solid curve is a fit to a single exponential and gives a time constant of 6.9 ± 0.3 ns. The result $g^{(2)}(t = 0) = 0.22$ confirms that the levitated-QD is a single-photon source.

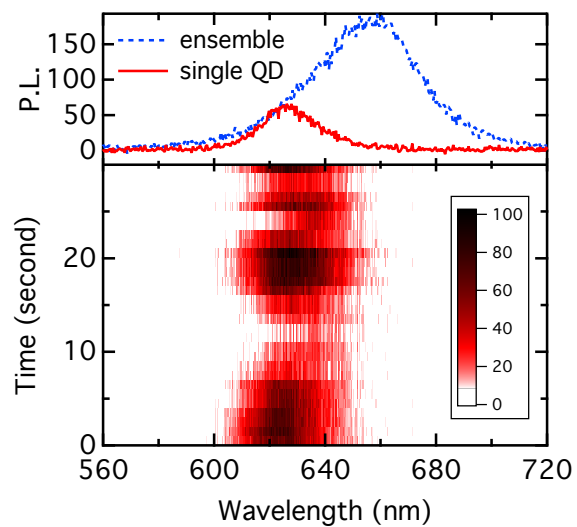


Figure 3 | Spectral fluctuations in fluorescence from levitated QD. (lower panel) Time-dependent fluorescence spectra from a single levitated QD. Integration was 1 s. (upper panel) The red curve is a typical fluorescence spectrum extracted from the lower panel at $t = 5$ s. For reference, the dotted blue curve shows the fluorescence spectrum from the QD ensemble.

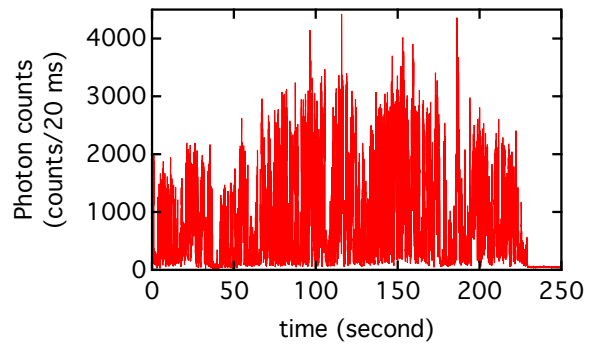


Figure 4 | Dynamics of fluorescence intensity. Time-dependent fluorescence intensity detected by an avalanche photodiode with 20 ms bin time. Optical levitation starts at $t \sim -70$ sec.